DOI: 10.17516/1997-1397-2021-14-1-105-116
УДК 548.0:534+004.942

Influence of Uniaxial Pressure on the Characteristics of Lamb and SH-wave Propagation in $LiNbO_3$ Crystalline Plates

Sergey I. Burkov*
Oleg N. Pletnev
Siberian Federal University
Krasnoyarsk, Russian Federation
Pavel P. Turchin†
Siberian Federal University
Krasnoyarsk, Russian Federation
Kirensky Institute of Physics, Federal Research Center KSC SB RAS
Krasnoyarsk, Russian Federation
Olga P. Zolotova‡
Reshetnev Siberian State University of Science and Technology
Krasnoyarsk, Russian Federation
Boris P. Sorokin§
Technological Institute for Superhard and Novel Carbon Materials
Moscow, Troitsk, Russian Federation

Received 12.09.2020, received in revised form 22.10.2020, accepted 15.11.2020

Abstract. Theoretical study of uniaxial pressure influence on the propagation characteristics of Lamb and SH-waves in lithium niobate plate is carried out. Electromechanical coupling coefficients and controlling coefficients of the pressure influence on phase velocity are calculated in various directions. Transformation and hybridization of acoustic modes upon a pressure influence have been derived in details.
PACS: 43.25.Fe; 43.35.Cg; 77.65.-j

Keywords: piezoelectric plate, Lamb wave, SH-wave, uniform pressure influence, computer simulation.

Citation: S.I. Burkov, O.N. Pletnev, P.P. Turchin, O.P. Zolotova, B.P. Sorokin, Influence of Uniaxial Pressure on the Characteristics of Lamb and SH Wave Propagation in $LiNbO_3$ Crystalline Plates, J. Sib. Fed. Univ. Math. Phys., 2021, 14(1), 105–116. DOI: 10.17516/1997-1397-2021-14-1-105-116.

Introduction

Studies of the propagation of the normal elastic waves in piezoelectric plates known as Lamb wave (LW) modes have been carried out for a quite some time [1, 2]. Note, that in practice the Lamb waves have some advantage in comparison with Rayleigh surface acoustic waves (SAW) owing to a smaller acoustic attenuation at microwave band and keeping a convenient possibility

*sburkov@sfu-kras.ru
†pturchin@sfu-kras.ru
‡zolotova@sibsau.ru https://orcid.org/0000-0003-2927-4278
§bpsorokin1953@yandex.ru

of excitation by an interdigital transducer (IDT). The influence of external static impacts on LW characteristics in the piezoelectric plates of PLZT ceramics and Y-cut of the lithium niobate crystal (LNC) was studied in [3,4], where the prospect of LW application in such devices as sensors of an electric field **E** as well as the **E**-controlled delay lines was studied. It was noted, that the sensitivity of LW based devices was the better than that based on Rayleigh wave propagation.

The **E**-influence on the characteristics of symmetric and antisymmetric Lamb waves in piezoelectric plates was theoretically studied in [5, 6]. However, this study was carried out in the framework of a perturbation theory without taking into account the nonlinear material tensors of a crystal. An experimental and theoretical study of the **E**-influence on the quasishear horizontal (QSH) wave propagated on the thin LNC plate of X, Y, and Z-cuts was performed in [7, 8], where promising directions of an elastic wave propagation in creating signal processing devices were obtained.

A detailed study of the **E**-influence on the characteristics of the fundamental (zero) LW mode in thin LNC plates was performed in [9, 10], where a strong dispersion dependence of LW phase velocity vs an electric field was marked. It was noted, that in this case an **E**-influence on the phase velocity has a substantial dependence *vs* the frequency, thus such dependence for some directions of the wave propagation could be changed from the linear to the quadratic one by varying the frequency [11].

Based on the LNC plate the high-quality acoustic resonator tuned by an electric field was demonstrated in [12]. General theory of the SAW propagation in a piezoelectric crystal as well as the reflection and refraction of elastic waves on the interface between two elastic media subjected to the pressure, was considered in [13, 14]. The **E**-influence on LW propagation in piezoelectric plates taking as an example of silicosillenite piezoelectric crystals was considered in detail in [15, 16].

Changes in the material properties of a crystal under an influence of uniform mechanical pressure studied in [17, 18], were used in stabilizing the resonance frequency and, in particular, compensating the frequency drift of the acoustic resonators based on langasite and quartz crystals [19, 20]. The influence of an initial stress on Love wave propagation in the piezoelectric layered structures (PLS) as "piezoelectric layer/isotropic substrate" and "isotropic layer/piezoelectric substrate" has been studied in a number of works [21, 22].

The aim of the present paper is concerned with a numerical analysis of an influence of uniaxial mechanical pressure on the characteristics of symmetric and antisymmetric Lamb waves as well as SH-waves taking the LNC plates as an example and including into consideration the complete set of the LNC non-linear electromechanical constants.

1. Theory of elastic wave propagation in piezoelectric plates under uniform pressure influence

Starting equation of motion for small amplitude waves, as well as the equations of electrostatics and the state equations of the piezoelectric medium subjected the influence of uniform mechanical pressure have obtained earlier [23] as

$$\begin{aligned} &\rho_0 \ddot{\tilde{U}}_A = \tilde{\tau}_{AB,B} + \tilde{U}_{A,PQ}\bar{\tau}_{PQ}; \qquad \tilde{D}_{M,M} = 0; \\ &\tilde{\tau}_{AB} = C^*_{ABCD}\tilde{\eta}_{CD} - e^*_{MAB}\tilde{E}_M; \qquad \tilde{D}_M = \varepsilon^*_{MN}\tilde{E}_N + e^*_{MAB}\tilde{\eta}_{AB}. \end{aligned} \tag{1}$$

In Eq. (1) the following notations are introduced: ρ_0 is the density of a crystal in the unde-

formed (initial) state, $\tilde{U}_A$ is the vector of dynamical elastic displacements, τ_{AB} is the tensor of a thermodynamic stress, $\tilde{D}_M$ is the electric displacement field vector, $\bar{\tau}_{PQ} = -\bar{\tau} P_P P_Q$ is the static uniaxial stress tensor, P_Q is the unit vector of a pressure force, and η_{CD} is the strain tensor. It was assumed that the compression stress should have a negative sign. Here and after the time-dependent variables are marked by "tilde" symbol. The comma after the subscript denotes a spatial derivative, and coordinate Latin indices vary from 1 to 3. Here and further, the rule of summation over repeated indices will be used.

Effective elastic, piezoelectric and dielectric constants in the approximation of a linear dependence on the magnitude of static mechanical stress $\bar{\tau}$ were defined in [24] as:

$$\begin{aligned} C^*_{ABKL} &= C^E_{ABKL} - C^E_{ABKLQR} S^E_{QRMN} P_M P_N \bar{\tau}; \\ e^*_{NAB} &= e_{NAB} - e_{NABKL} S^E_{KLMN} P_M P_N \bar{\tau}; \\ \varepsilon^*_{MN} &= \varepsilon^\eta_{MN} - H_{NMAB} S^E_{ABKL} P_K P_L \bar{\tau}. \end{aligned} \tag{2}$$

Here C^E_{ABKL}, e_{NAB}, and ε^η_{MN} are the second-order elastic, piezoelectric and dielectric constants, respectively; S^E_{ABKL} is the tensor of elastic compliances; C^E_{ABKLQR}, e_{NABKL}, and H_{NMAB} are the third-order elastic, nonlinear piezoelectric and electrostrictive material tensors, respectively.

Substituting into Eq. (1) the solutions for the elastic displacements and electric potential in a conventional form of the plane monochromatic waves, one can obtain the linearized Green-Christoffel equations as:

$$\begin{aligned} &\left[\Gamma_{BC}\left(\bar{\tau}\right) - \rho_0 \omega^2 \delta_{BC}\right] \alpha_C = 0; \\ &\Gamma_{BC} = \left[C^*_{ABCD} + \left(2 C^E_{MBFN} S^E_{ADCF} + \delta_{BC}\delta_{AM}\delta_{DN}\right) P_M P_N \bar{\tau}\right] k_A k_D; \\ &\Gamma_{C4} = e^*_{PAC} k_P k_A; \qquad \Gamma_{4C} = \Gamma_{C4} + 2 e_{AFD} S^E_{MNCF} P_M P_N \bar{\tau} k_A k_D; \\ &\Gamma_{44} = -\varepsilon^*_{PQ} k_P k_Q. \end{aligned} \tag{3}$$

Here k_A is an acoustic wave vector.

Let the X_3 axis of an operational coordinate system is directed along the outer normal to the surface of the plate, occupying the $0 \leqslant X_3 \leqslant h$ space, and the X_1 axis coincides with the wave propagation direction. Here h is the plate thickness.

The propagation of an elastic wave in a piezoelectric layered structure under a uniform pressure must satisfy to the corresponding boundary conditions. The boundary condition for the normal components of a stress tensor is that their equality to zero of the layer should be fulfilled on the free surface. The continuity of the tangential components of an electric field is ensured by the conditions on the continuity of the electric potential φ as well as the normal component of an electrical displacement vector at a crystal-vacuum interface. All such conditions can be written as:

$$\begin{aligned} &\tau_{3A} = 0|_{X_3=h}\,; \qquad D_3 = D^{vac}|_{X_3=h}\,; \qquad \varphi_3 = \varphi|_{X_3=h}\,; \\ &\tau_{3A} = 0|_{X_3=0}\,; \qquad D_3 = D^{vac}|_{X_3=0}\,; \qquad \varphi_3 = \varphi|_{X_3=0}\,. \end{aligned} \tag{4}$$

In the case of mechanical stress application orthogonally the free surface ($\mathbf{P} \parallel X_3$) the elastic properties of a loading medium must be taken into account. Assuming that a uniaxial stress in such geometry occurs without a hard contact with a free surface specimen, for example, by means of gaseous static equipment, the mechanical boundary conditions can be written in the form [24]:

$$\tilde{\tau}_{3J} + \tilde{\mathrm{U}}_{J,K} \bar{\tau}_{3K} = 0 \quad (X_3 = h)\,. \tag{5}$$

Substituting the solutions in a conventional form of plane homogeneous waves into the Eq. (4), one can obtain a system of equations for calculating the propagation parameters of acoustic waves in a piezoelectric plate as:

$$\begin{aligned}
&\sum_{n=1}^{8}\left[a_n\left(e^*_{3AB}+2S^E_{ABKP}e_{3AB}P_KP_P\bar{\tau}\right)k_B^{(n)}\alpha_A^{(n)}+\left(\varepsilon^*_{3K}k_K^{(n)}-i\varepsilon_0\right)\alpha_4^{(n)}\right]\exp(ik_3^{(n)}h)=0;\\
&\sum_{n=1}^{8}\left[a_n\left(C^*_{B3KL}+2S^E_{KPMN}C^E_{3BKL}P_MP_N\bar{\tau}\right)k_L^{(n)}\alpha_P^{(n)}-e^*_{P3B}k_P^{(n)}\alpha_4^{(n)}\right]\exp(ik_3^{(n)}h)=0;\\
&\sum_{n=1}^{8}a_n\left(C^*_{B3KL}+2S^E_{KPMN}C^E_{3BKL}P_MP_N\bar{\tau}\right)k_L^{(n)}\alpha_P^{(n)}-e^*_{P3B}k_P^{(n)}\alpha_4^{(n)}=0;\\
&\sum_{n=1}^{8}a_n\left(e^*_{3AB}+2S^E_{ABKP}e_{3AB}P_KP_P\bar{\tau}\right)k_B^{(n)}\alpha_A^{(n)}+\left(\varepsilon^*_{3N}k_N^{(n)}+i\varepsilon_0\right)\alpha_4^{(n)}=0.
\end{aligned}\tag{6}$$

Here $\alpha_K^{(n)}$, a_n, and $k_L^{(n)}$ designate the amplitudes, weight coefficients and wave numbers of the nth partial wave ($n = 1, \ldots, 8$) in the crystalline plate, respectively.

In Eqs. (6), all the changes in the configuration of an anisotropic continuous medium associated with its static deformation and, in particular, with changes in the shape of a specimen (so-called geometric non-linearity), as well as the changes in the material constants (see Eq. (2)) of a piezoelectric crystal (so-called physical non-linearity) under the influence of hard mechanical stress have been taken into account. Final system of boundary conditions has 8 homogeneous equations relatively the unknown weight coefficients a_n. The calculation of elastic wave parameters was carried out using a conventional method of partial waves [23]. The equality to zero of the determinant of boundary condition matrix was used to obtain a required Lamb wave phase velocity.

2. Dispersion dependences of Lamb and SH-wave propagation parameters

Based on Eqs. (1)–(6), a computer calculation of such parameters of Lamb and SH-waves as phase velocities, electromechanical coupling coefficients (EMCCs), controlling coefficients of phase velocities for LNC plate under a lot of uniform mechanical stress was carried out. Electromechanical coupling coefficients were calculated by a conventional relation:

$$K^2 = 2\frac{(v - v_m)}{v},\tag{7}$$

where the phase velocities v and v_m should be defined at free or shorted surface boundary conditions, respectively. Controlling coefficients of the phase velocity upon application of an uniaxial pressure were taken in the form:

$$\alpha_P = \frac{1}{v(0)}\left(\frac{\Delta v}{\Delta P}\right)_{\Delta P\to 0}.\tag{8}$$

Here the value P is the pressure magnitude. Data on the linear and nonlinear electromechanical properties for the $LiNbO_3$ crystal were taken from [25].

Fig. 1 represents the dispersion dependences of the phase velocities, EMCCs, and α_P controlling coefficients in the [100] direction of a wave propagation for the (001) plate orientation and 3 kinds of an uniaxial pressure application along the [100], [010], and [001] directions. The

range of the hf product considered was varied from 0 up to 16000 m/s. Analyzing Fig. 1 (a) one can see that the phase velocity curves of the symmetric S_0 and antisymmetric A_0 modes tend to Rayleigh wave phase velocity at an elevated frequency as well as a large-scale plate thickness. At the same conditions, the dispersive phase velocity of the SH_0 mode tends to an appropriate value of the bulk acoustic wave (BAW) of quasishear type which has a phase velocity with comparatively slow value (so-called QSS wave). Fig. 1 (b) shows that all the considered modes have non-zero electromechanical coupling, but the maximum value for the fundamental (zero) modes is achieved for the SH_0 mode as $K^2 = 0.15$ for comparatively thin plates at $hf = 250$ m/s, while for the symmetric mode S_0, the EMCC values have a much lower magnitude as $K^2 = 0.014$, which is consistent with work [26]. It should be noted that in the LNC plates the hybridization of elastic modes [27] occurs mainly at the intersection points of dispersion curves. However, when one of free surface has a metallization, the dispersion curves break apart and the mode types will change [15, 28]. But a similar effect doesn't occur upon a metallization of both free surfaces of a plate. The first modes of Lamb and SH_1 waves have large EMCC values (Fig. 1 (b)) in comparison with the zero modes.

The maximum value of the controlling coefficient $\alpha_P = 2.13 \cdot 10^{-11}$ Pa^{-1} at $hf = 2200$ m/s for LW fundamental modes is achieved for the S_0 mode when $\mathbf{P} \parallel [100]$, i.e. along the propagation direction (Fig. 1 (c)). But the maximal α_P value of the A_0 mode is somewhat higher. So, for $hf = 6050$ m/s values it becomes equal to $2.37 \cdot 10^{-11}$ Pa^{-1}. But at $hf \geqslant 8000$ m/s the α_P coefficient becomes equal to $2.25 \cdot 10^{-11}$ Pa^{-1} coinciding with the similar value calculated for non-dispersive Rayleigh wave. This can be explained by the transformation of the S_0 mode into Rayleigh type at a higher frequency. The α_P dispersion dependence of the SH_0 mode increases monotonously when $hf > 6500$ m/s, and tends to the appropriate value observed for the QSS BAW as $3.01 \cdot 10^{-11}$ Pa^{-1}. The range of the changes in the α_P values observed for higher-order elastic Lamb modes is significantly larger. For example, this fact can be quite seen for the S_1 symmetrical mode where the maximal $3.02 \cdot 10^{-11}$ and minimal $6.9 \cdot 10^{-12}$ Pa^{-1} α_P values are realized at $hf = 3450$ and 15450 m/s, respectively.

In the case of $\mathbf{P} \parallel [010]$, i.e. orthogonally to the sagittal plane and propagation direction, the maximal value of $\alpha_P = 1.56 \cdot 10^{-11}$ Pa^{-1} at $hf = 2800$ m/s is achieved for the S_0 mode in the vicinity of the S_0 and SH_1 hybridization (Fig. 1 (d)). Hybridization effect which consists in the existence of coupled modes and energy exchange under the conditions of space-time synchronism, is displayed on the behavior of the α_P coefficients, which in this case can serve as a qualitative parameter of a hybridization level. In particular, the $\mathbf{P}$ application along the direction [010] increases the interaction area of the S_0 and SH_1 modes as in the case of a slight change in the propagation direction of the elastic wave as shown in [27]. For the SH_0 mode, the maximal value of $\alpha_P = 2.66 \cdot 10^{-11}$ Pa^{-1} at $hf = 5600$ m/s. The maximal values of $\alpha_P = 2.27 \cdot 10^{-11}$ and $4.51 \cdot 10^{-11}$ Pa^{-1} for the S_1 and S_2 modes are realized at $hf = 15900$ and 4100 m/s, respectively. The dispersive dependences of the α_P coefficients of SH_1 and SH_2 modes are distinguished sufficiently, because when the hf product increases, the α_P for the SH_1 similarly the SH_0 mode tends to appropriate value of QSS BAW mode, but the α_P coefficient for the SH_2 tends to appropriate value of the QFS BAW mode as $2.96 \cdot 10^{-11}$ Pa^{-1}. Note that for some modes the α_P coefficients are equal to zero, i.e. an application of uniaxial mechanical pressure does not affect on their phase velocities. For example, this is fulfilled for the SH_0 mode at $hf = 10250$ m/s as well as for the S_0 mode at $hf = 4300$ m/s.

Fig. 1 (e) represents the dispersive dependencies of the α_P coefficient when uniaxial mechanical pressure is applied along the normal to free surface of a plate, i.e. along the threefold axis

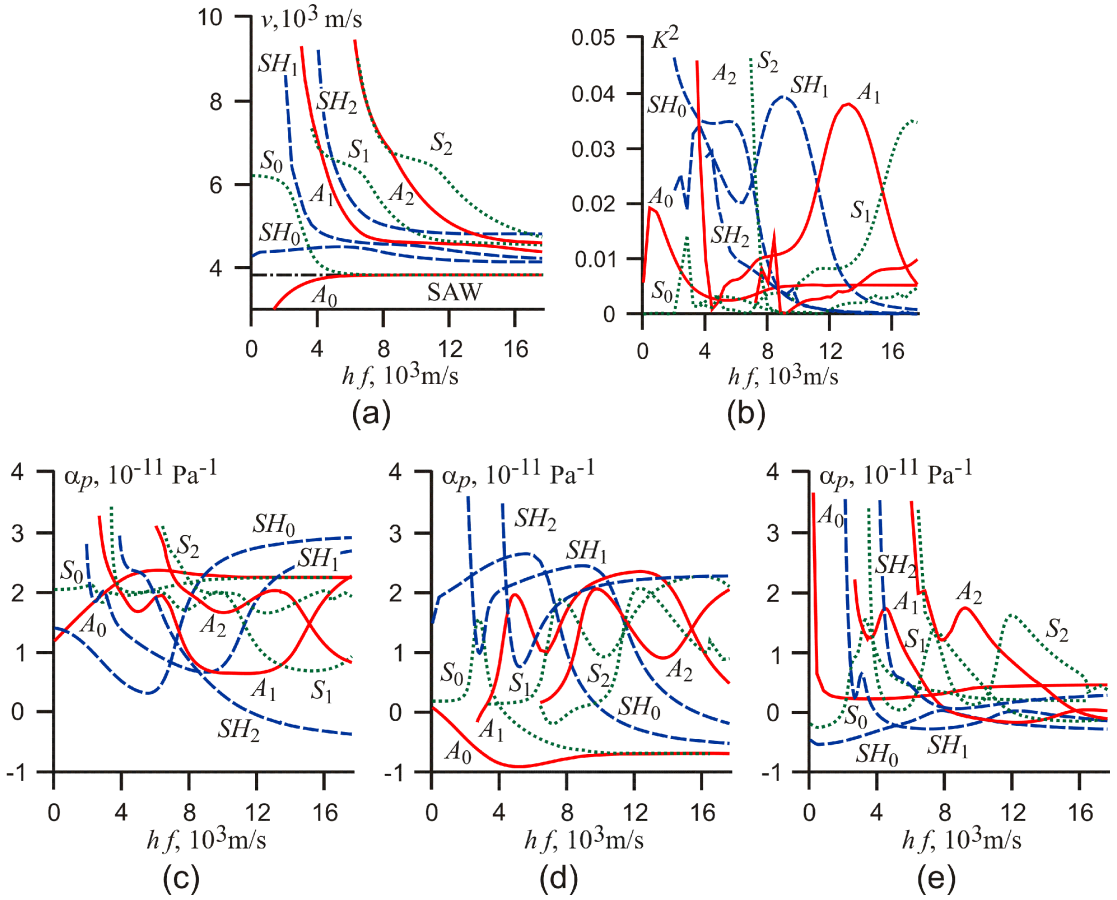

Fig. 1. Dispersion dependences of the parameters of Lamb and SH-waves in Z-cut of lithium niobate crystal plate. (a) Phase velocities; (b) EMCCs when one side of a plate was metalized; (c) α_P controlling coefficients at $\mathbf{P} \parallel [100]$; (d) α_P controlling coefficients at $\mathbf{P} \parallel [010]$; (e) α_P controlling coefficients at $\mathbf{P} \parallel [001]$. Red curves should be associated with the A_n modes, dashed green ones with the S_n modes, and dashed blue ones with the SH_n modes

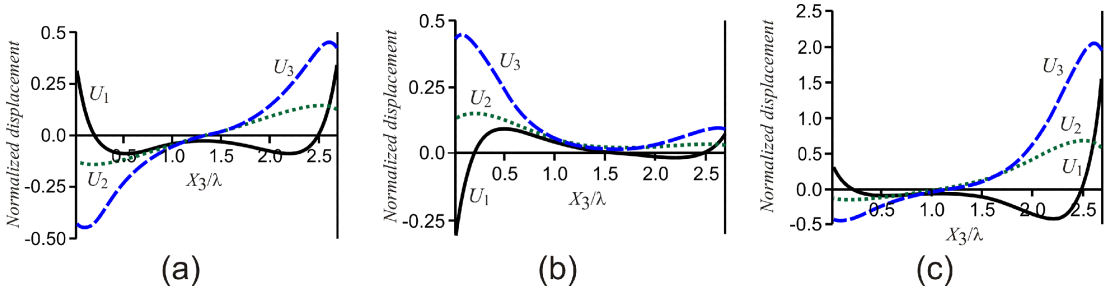

Fig. 2. Normalized components of the displacement vectors of the A_0 and S_0 modes in lithium niobate plate at $hf = 10250$ m/s. (a) S_0 mode at $\mathbf{P} = 0$; (b) A_0 mode at $\mathbf{P} \parallel [001]$; (c) S_0 mode at $\mathbf{P} \parallel [001]$

[001]. A significant increasing in the α_P coefficients of the A_0 mode is observed at small values of hf product, in particular $\alpha_P = 6.45 \cdot 10^{-11}$ Pa^{-1} at $hf = 50$ m/s. For the SH_0 mode at $hf > 5500$ m/s there is a monotonous growth of the α_P coefficient tending the appropriate value obtained under the same conditions for the QSS BAW as $\alpha_P = 3.6 \cdot 10^{-12}$ Pa^{-1}. The behavior of the α_P dispersion dependence of the higher order modes as A_2, and SH_2 is basically the same as in the case of **P** application orthogonally to the sagittal plane, considered above. The values of the α_P coefficients of the A_2 and SH_2 modes at $hf = 12000$ m/s are $1.63 \cdot 10^{-11}$ and $4.4 \cdot 10^{-13}$ Pa^{-1}, respectively.

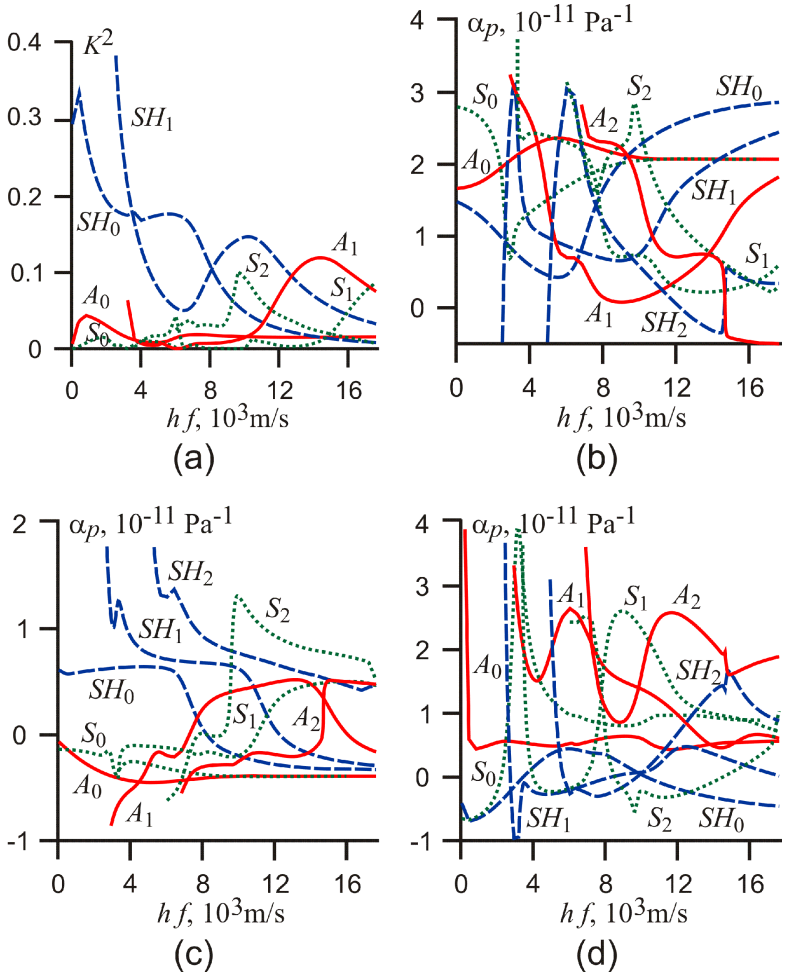

Fig. 3. Dispersive dependencies of the parameters of Lamb and SH-waves propagating [100] direction in the LNC Y-cut under the uniaxial pressure application. (a) EMCCs; (b) α_P coefficients at **P** ||[100]; (c) α_P coefficients at **P** ||[001]; (d) α_P coefficients at **P** ||[010]. Red curves should be associated with the A_n modes, dashed green ones with the S_n modes, and dashed blue ones with the SH_n modes

When the uniaxial pressure **P** ||[001] is applied along the normal to a free plate surface, one can observe a peculiarity in the behavior of Lamb fundamental modes. Fig. 2 represents the normalized components of displacement vector for A_0 and S_0 modes at $hf = 10250$ m/s. In the case without the pressure influence, the A_0 and S_0 modes at $hf > 9000$ m/s degenerate into

Rayleigh surface wave with the phase velocity as 3823.66 m/s. Elastic displacements in the A_0 and S_0 fundamental modes have a maximal value on the free surfaces and are practically equal to zero in the middle plane of a crystalline plate (Fig. 2 (a)) [1]. Application of the uniaxial pressure at $\mathbf{P} \parallel [001]$ leads to removing an above mentioned degeneration and splitting Rayleigh SAW mode back into the A_0 and S_0 modes. The displacements of Lamb modes A_0 and S_0 are concentrated at the lower and upper free surface of the plate, respectively (Figs. 2 (b), 2 (c)). If the S_0 mode is transformed into the SAW mode with the phase velocity $v_R = 3822.39$ m/s at $\mathbf{P} = 10^8$ Pa and $\alpha_P = 1.93 \cdot 10^{-12}$ Pa^{-1}, then the mode A_0 has the phase velocity $v_{A_0} = 3821.38$ m/s and $\alpha_P = 4.54 \cdot 10^{-12}$ Pa^{-1} (Fig. 1 (e)).

On Fig. 3 the values of EMCCs and α_P coefficients of Lamb and SH modes propagating in the [100] direction of Y-cut upon an application of uniaxial mechanical pressure are represented. In this case all the modes have a piezoelectric activity (Fig. 3 (a)). The maximal EMCC values are achieved for the S_0 mode as $K^2 = 0.35$ at $hf = 7060$ m/s and for SH_0 mode as $K^2 = 0.39$ at $hf = 450$ m/s. In the case when uniaxial pressure is applied along the wave propagation direction $\mathbf{P} \parallel [100]$, a series of interactions between the modes also arise, in particular, between S_0 and SH_1, S_1 and SH_2, as well as between the A_2 and SH_2 modes. This reflects in a behavior of α_P coefficients (Fig. 3 (b)). For example, in the interaction region between the S_0 and SH_1 modes at $hf = 3200$ m/s the changes in α_P coefficients realize within the range of $2.6 \cdot 10^{-11}$ up to $7.04 \cdot 10^{-12}$ Pa^{-1}, and of $3.41 \cdot 10^{-12}$ up to $3.11 \cdot 10^{-11}$ Pa^{-1}, respectively.

When uniaxial pressure $\mathbf{P} \parallel [001]$ is applied orthogonally to the sagittal plane of Y-cut, the α_P values of almost all modes are sufficently smaller than those in the case $\mathbf{P} \parallel [100]$ considered above. Additionally there are the zero α_P coefficients for some modes (Fig. 3 (c)).

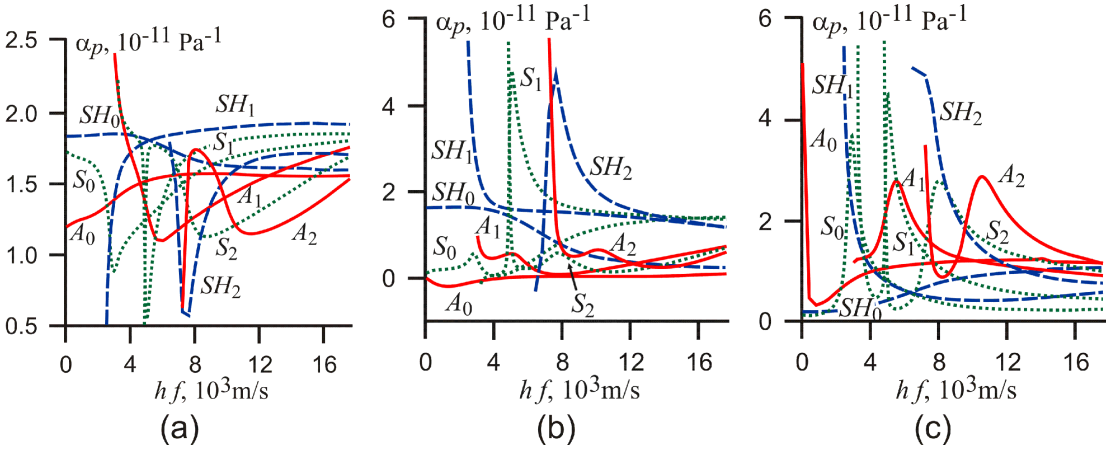

Fig. 4. Dispersive dependences of the controlling coefficients in Lamb and SH modes propagating [001] direction in LNC X-cut under an application of uniaxial pressure. (a) α_P coefficients at $\mathbf{P} \parallel [001]$; (b) α_P coefficients at $\mathbf{P} \parallel [010]$; (c) α_P coefficients at $\mathbf{P} \parallel [100]$. Red curves should be associated with the A_n modes, dashed green ones with the S_n modes, and dashed blue ones with the SH_n modes

When the pressure is applied along the normal to free surface $\mathbf{P} \parallel [010]$, a significant increase in α_P coefficient of mode A_0 at small hf values takes place. In particular, $\alpha_P = 6.7 \cdot 10^{-11}$ Pa^{-1} at $hf = 50$ m/s (Fig. 3 (c)). Similarly, a "splitting" of the phase velocities for the A_0 and S_0 modes occurs. If $\mathbf{P} = 0$, at $hf > 9000$ m/s the fundamental modes A_0 and S_0 degenerate into Rayleigh wave with the phase velocity $v_{SAW} = 3798.8$ m/s. Upon the P application the A_0 mode

degenerates into Rayleigh wave with the vSAW = 3796.7 m/s and $\alpha_P = 5.63 \cdot 10^{-12}$ Pa^{-1}, then the S_0 mode has the phase velocity $v_{S_0} = 3795.44$ m/s and $\alpha_P = 8.54 \cdot 10^{-12}$ Pa^{-1}.

It should be noted that the controlling coefficients grow significantly in the region of interaction between the S_0 and SH_1 modes, $\alpha_P = 3.99 \cdot 10^{-11}$ and $-1.08 \cdot 10^{-11}$ Pa^{-1}, respectively (Fig. 3 (d)).

On Fig. 4 the dispersive dependences of the α_P coefficients for Lamb and SH modes which propagate along the [001] direction in LNC X-cut upon the **P** application are presented. In this case, in particular, the A_0 and S_0 fundamental Lamb modes don't degenerate now into the SAW mode in all the considered range of the hf variation at all the variants of **P** application. When uniaxial pressure is applied along the propagation direction as **P** ‖[001], the α_P coefficients of the A_0 and SH_0 modes tend to the appropriate value $\alpha_P = 1.57 \cdot 10^{-11}$ Pa^{-1} observed in the SAW mode, but α_P coefficient of the S_0 mode tends to $1.8 \cdot 10^{-11}$ Pa^{-1} value as the QSS BAW mode (Fig. 4 (a)). Note, that only at **P** ‖[001] there are zero values of the α_P coefficients. Application of an uniaxial pressure **P** ‖[100] significantly increases the hybridization effect between the S_0 and SH_1 modes. In particular, for the S_0 and SH_1 modes the value of the α_P coefficients are $3.7 \cdot 10^{-11}$, and $2.4 \cdot 10^{-11}$ Pa^{-1}, respectively (Fig. 4 (c)).

The extremal values of α_P coefficients are summarized in the Tab. 1.

Table 1. Extremal values of α_P coefficients for Lamb and SH modes in lithium niobate

Cut	Mode	Pressure force direction	hf, m/s	Phase velocity, m/s	α_P, $^{-11}$ Pa^{-1}
Z-cut	A_1	[100]	2800	10271.4	3.02
	S_2		11600	4838.07	0
	SH_2	[010]	6050	8483.2	3.65
	S_0		4300	4022.26	0
	SH_0		5600	4492.4	2.66
	SH_0		10300	4229.1	0
	S_0	[001]	1950	6031.8	0
	A_1		4500	6376.1	1.75
	S_3		9200	6276.1	1.74
	SH_0		7650	4401.06	0
Y-cut	SH_2	[100]	12250	4860.7	0
	A_0		5600	3778.7	2.36
	S_0		1250	6663.9	2.67
	S_0	[010]	3150	5079.5	3.99
	SH_0		3450	4536.5	0
X-cut	A_0	[010]	4600	3434.9	0
	S_1		5050	6708.7	4.81
	S_0	[100]	2950	5257.1	3.68
	A_1		5000	6710.8	4.5

3. Conclusion

Using the general results obtained in the Section 3, one can analyze in detail the dispersion of the main parameters for different acoustic modes in a piezoelectric plate under an application of uniaxial pressure. A prerequisite for this analysis is the knowledge of all the linear and nonlinear electromechanical constants of a crystal.

Dispersive dependences of the phase velocities, EMCCs, α_P controlling coefficients *vs* the hf

product for the X-, Y- and Z-cuts of lithium niobate single crystals under the homogeneous uniaxial pressure applied in a lot of directions have been calculated. It should note the highest values of α_P coefficients for the mode A_0 in the thin plates, for example, $\alpha_P = 5.13 \cdot 10^{-11}$, $6.7 \cdot 10^{-11}$, and $6.4 \cdot 10^{-11}$ Pa^{-1} at $hf = 50$ m/s in the X-, Y- and Z-cuts, respectively. It has been demonstrated that for various applications of uniaxial mechanical pressure, the interaction of elastic wave modes can occur. Such kind of study can be usefull for the physical acoustics as well as in point of view in the practical applications, for example in acoustic sensors based on Lamb or SH-waves.

This work was supported by the grant of the Russian Science Foundation (project # 16-12-10293).

References

[1] I.A.Viktorov, Rayleigh and Lamb waves: physical theory and applications, Plenum Press, New York, 1967.

[2] G.W.Farnell, Properties of elastic surface waves: in: W.P. Mason, R.N. Thurston (Eds.), Physical Acoustics – Principles and Methods, Academic Press, New York, London, 1970, 109–166.

[3] K.Toda, K.Mizutani, A Lamb wave voltage sensor, *J. Acoust. Soc. Am.*, **74** (1983), 677–679.

[4] A.Palma, L.Palmieri, G.Socino, E.Verona, Lamb wave electroacoustic voltage sensor, *J. Appl. Phys.*, **58**(1985), 3265–3267.

[5] H.Liu, T.J.Wang, Z.K.Wang, Z.B.Kuang, Effect of a biasing electric field on the propagation of antisymmetric Lamb waves in piezoelectric plates, *Int. J. Solids Struct.*, **39**(2002), 1777–1790.

[6] H.Liu, T.J.Wang, Z.K.Wang, Z.B.Kuang, Effect of a biasing electric field on the propagation of symmetric Lamb waves in piezoelectric plates, *Int. J. Solids Struct.*, **39**(2002), 2031–2049.

[7] S.G.Joshi, B.D.Zaitsev, I.E.Kuznetsova, SH acoustic waves in a lithium niobate plate and the effect of electrical boundary conditions on their properties, *Acoust. Phys.*, **47**(2001), 282–285.

[8] B.D.Zaitsev, I.E.Kuznetsova, S.G.Joshi, Theoretical and experimental investigation of QSH (quasi shear horizontal) acoustic waves, *Ultrasonics*, **36**(1998), 31—35.

[9] B.D.Zaitsev, I.E.Kuznetsova, Electric field influence on acoustic waves, *Handbook of Advanced Electronic and Photonic Materials and Devices*, (2001). Ed. H.S. Nalwa, 139–174. DOI: 10.1016/B978-012513745-4/50039-1.

[10] B.D.Zaitsev, S.G.Joshi, I.E.Kuznetsova, Electric-field influence on Lamb and SH wave properties in $LiNbO_3$ plates, *J. Acoust. Soc. Am.*, **103**(1998), 2883.

[11] B.D.Zaitsev, V.Yu.Kalinin, I.E.Kuznetsova, Nonlinear electroacoustic interaction for elastic waves in lithium niobate plates, *Acoust. Phys.*, **45**(1999), 196—201.

[12] H.Zhang, J.A.Turner, J.Yang, J.A.Kosinski, Electroelastic effect of thickness mode langasite resonators, *IEEE TUFFC*, **54**(2007), 2120–2128.

[13] S.I.Burkov, B.P.Sorokin, K.S.Aleksandrov, A.A.Karpovich, Reflection and refraction of bulk acoustic waves in piezoelectrics under uniaxial stress, *Acoust. Phys.*, **55**(2009), 178–185.

[14] S.I.Burkov, B.P.Sorokin, A.A.Karpovich, K.S.Aleksandrov, Reflection and refraction of bulk acoustic waves in piezoelectric crystals under the action of bias electric field and uniaxial pressure, *Proc. Ultras. Symp*, IEEE, (2008), 2161–2164.

[15] S.I.Burkov, Z O.P.olotova, B.P.Sorokin, Al K.S.eksandrov, Effect of external electrical field on characteristics of a Lamb wave in a piezoelectric plate, *Acoust. Phys.*, **56**(2010), 644–650.

[16] S.I.Burkov, O.P.Zolotova, B.P.Sorokin, Influence of the external electric field on propagation of the lamb waves in the piezoelectric plates, *IEEE TUFFC*, **58**(2011), 239–243.

[17] F.Kubat, W.Ruile, T.Hesjedal, J.Stotz, U.Rosler, L.M.Reindl, Calculation and experimental verification of the acoustic stress at GHz frequencies in SAW resonators, *IEEE TUFFC*, **51**(2004), 1437–1448.

[18] Y.Jing, J.Chen, X.Gong, J.Duan, Stress-induced frequency shifts in rotated Y-cut langasite resonators with electrodes considered, *IEEE TUFFC*, **54**(2007), 906–909.

[19] J.A.Kosinski, Jr. R.A.Pastore, J.Yang, X.Yang, J.A.Turner, Stress-induced frequency shifts of degenerate thickness-shear modes in rotated Y-cut quartz resonators, *IEEE TUFFC*, **57**(2010), 1880–1883.

[20] J.A.Kosinski, Jr. R.A.Pastore, X.Yang, J.Yang, J.A.Turner, Stress-induced frequency shifts in langasite thickness-mode resonators, *IEEE TUFFC*, **56**(2009), 129–135.

[21] H.Liu, Z.K.Wang, T.J.Wang, Effect of initial stress on the propagation behavior of Love waves in a layered piezoelectric structure, *Int. J. Solids Struct.*, **38**(2001), 37–51.

[22] Z.Qian, F.Jin, Z.Wang, K.Kishimoto, Love waves propagation in a piezoelectric layered structure with initial stresses, *Acta Mech.*, **171**(2004), 41–57.

[23] K.S.Aleksandrov, B.P.Sorokin, S.I.Burkov, Effective piezoelectric crystals for acoustoelectronics, piezotechnics and sensors, Vol. 2, SB RAS Publishing House, Novosibirsk, 2008 (in Russian).

[24] S.I.Burkov, O.P.Zolotova, B.P.Sorokin, P.P.Turchin, The analysis of the effect of homogeneous mechanical stress on the acoustic wave propagation in the "$La_3Ga_5SiO_{14}$/fused silica" piezoelectric layered structure, *Ultrasonics*, **55**(2015), 104–112.

[25] Y.Cho, K.Yamanouchi, Nonlinear, elastic, piezoelectric, electrostrictive, and dielectric constants of lithium niobate, *J. Appl. Phys.*, **61**(1987), 875–887.

[26] I.E.Kuznetsova, B.D.Zaitsev, S.G.Joshi, I.A.Borodina, Investigation of acoustic waves in thin plates of lithium niobate and lithium tantalate, *IEEE TUFFC*, **48**(2001), 322–328.

[27] I.E.Kuznetsova, B.D.Zaitsev, A.A.Teplykh, I.A.Borodina, Hybridization of acoustic waves in piezoelectric plates, *Acoust. Phys.*, **53**(2007), 64–69.

[28] I.E.Kuznetsova, B.D.Zaitsev, I.A.Borodina, A.A.Teplykh, V.V.Shurygin, S.G.Joshi, Investigation of acoustic waves of higher order propagating in plates of lithium niobate, *Ultrasonics*, **42**(2004), 179–182.

Влияние одноосного механического давления на характеристики волн Лэмба и SH-волн в пластинах кристалла $LiNbO_3$

Сергей И. Бурков
Олег Н. Плетнев
Сибирский федеральный университет
Красноярск, Российская Федерация
Павел П. Турчин
Сибирский федеральный университет
Красноярск, Российская Федерация
Институт физики им. Л.В.Киренского ФИЦ КНЦ СО РАН
Красноярск, Российская Федерация
Ольга П. Золотова
Сибирский государственный университет науки и технологий им. Решетнева
Красноярск, Российская Федерация
Борис П. Сорокин
Технологический институт сверхтвердых и новых углеродных материалов
Москва, Троицк, Российская Федерация

Аннотация. Проведено теоретическое исследование влияния одноосного механического давления на характеристики распространения акустических волн в пластине ниобата лития. Рассчитаны коэффициенты электромеханической связи и коэффициенты управляемости при различных вариантах приложения внешнего механического одноосного давления.

Ключевые слова: пьезоэлектрическая пластина, волна Лэмба, SH-волна, влияние однородного давления, компьютерное моделирование.